

Crystal water induced switching of magnetically active orbitals in CuCl_2

M. Schmitt¹, O. Janson¹, M. Schmidt¹, S. Hoffmann¹, W. Schnelle¹, S.-L. Drechsler² and H. Rosner¹

¹*Max-Planck-Institut für Chemische Physik fester Stoffe, 01187 Dresden, Germany and*

²*IFW Dresden, P.O.Box 270116, 01171 Dresden, Germany*

The dehydration of $\text{CuCl}_2 \cdot 2\text{H}_2\text{O}$ to CuCl_2 leads to a dramatic change in magnetic behavior and ground state. Combining density functional electronic structure and model calculations with thermodynamical measurements we reveal the microscopic origin of this unexpected incident – a crystal water driven switching of the magnetically active orbitals. This switching results in a fundamental change of the coupling regime from a three-dimensional antiferromagnet to a quasi one-dimensional behavior. CuCl_2 can be well described as a frustrated J_1 – J_2 Heisenberg chain with ferromagnetic exchange J_1 and $J_2/J_1 \sim -1.5$ for which a helical ground state is predicted.

PACS numbers:

I. INTRODUCTION

Low-dimensional spin 1/2 magnets are of wide interest in solid state physics since they are ideal objects to study the interplay of dimensionality, magnetic frustration and strong quantum fluctuations. These compounds can be described often very successfully based on their magnetically active structural building blocks and their linking. Typical examples for such building blocks are Ti(III)O_6 octahedra, V(IV)O_5 square pyramids or Cu(II)O_4 plaquettes that form various spin 1/2 networks like quasi one-dimensional (1D) chains or ladders. Nevertheless, for a reliable and accurate description of such networks, precise model parameters are a precondition, especially in the vicinity of quantum critical points. However, since for new compounds these parameters are unknown, it is common to transfer the known parameters from related, similar systems in a slightly renormalized form according to changed distances and/or bond angles.

A typical example for the application of this strategy are compounds that contain crystal water in different amounts. Although in some cases the topology of the magnetic network and the related magnetic properties totally change upon dehydration like in the case of $\text{CuSiO}_3 \cdot \text{H}_2\text{O}$ ^{1,2} and CuSiO_3 ^{3,4}, for most compounds only moderate structural changes with respect to the magnetic network are observed. It is generally assumed that in this case crystal water leads mainly to a modest change of the crystal field for the magnetic ion. In turn, small changes in the crystal field only, would directly suggest a description within the same model with slightly revised parameters.⁵ This leads to the common belief that crystal water plays only a minor role regarding the magnetic properties for compounds where crystal structure is basically preserved upon water intercalation.

Here, in contrast, we show that the hydration of CuCl_2 to $\text{CuCl}_2 \cdot 2\text{H}_2\text{O}$ fundamentally changes the magnetic properties, although the topology of the covalent Cu-Cl network is seemingly unchanged. Whereas $\text{CuCl}_2 \cdot 2\text{H}_2\text{O}$ is a classical three-dimensional (3D) antiferromagnet (AFM) with a Néel temperature of 4.3 K, we establish the dehydrated species as an example for

a quasi 1D chain compound. The results of susceptibility measurements, density functional and model calculations can be consistently understood from a reorientation of the magnetically active Cu orbital driven by the hydration. Regarding the well known 3D magnetic nature of $\text{CuCl}_2 \cdot 2\text{H}_2\text{O}$,^{6,7} the quasi 1D behavior of the water free compound CuCl_2 is rather surprising: CuCl_2 is a J_1 – J_2 Heisenberg chain model compound with FM nearest neighbor (NN) exchange J_1 and AFM next-nearest neighbor (NNN) exchange J_2 . According to the estimated $J_2/J_1 \sim -1.5$ we predict a helical magnetic order below the observed transition at 24 K. Earlier studies^{8,9} that tried to model CuCl_2 as a spin 1/2 chain found considerable deviations from a 1D behavior since in these investigations only NN AFM coupling was considered. Alternatively a 1D model with AFM NN and NNN exchanges was suggested, but this model yields far too large couplings.¹⁰

II. CRYSTAL STRUCTURE

The crystal structure of CuCl_2 is presented in Fig. 1. Cu and Cl form a covalent network of edge shared CuCl_4 plaquettes running along b direction. Such fourfold planar Cu^{2+} coordination suggests a strong analogy to the undoped cuprates. The Cu-Cl-Cu bond angle is 93.6° and thus very similar to that in the CuO_2 chain cuprate family, where bond angles close to 90° result in FM NN exchange like in Li_2CuO_2 ,^{11,12} LiCu_2O_2 ^{13,14,15} and $\text{Li}_2\text{ZrCuO}_4$ ^{28,16}. As in the latter two compounds, these chains are arranged in layers (Fig. 1, top), suggesting a rather weak exchange between the layers. Since even the arrangement of the chains within the layers is very similar, a quasi 1D behavior might be expected from a mere comparison with these cuprate crystal structures.

When CuCl_2 is exposed to moisture, H_2O enters the space between the chain layers, finally forming the fully hydrated $\text{CuCl}_2 \cdot 2\text{H}_2\text{O}$ (Fig. 1, bottom). Although the crystal structure seems very similar at a first glance, the crystal water induces several changes: (i) The inter-layer distance increases, (ii) the CuCl_2 chains shift with respect to each other and, (iii) the Cu-Cl distances within

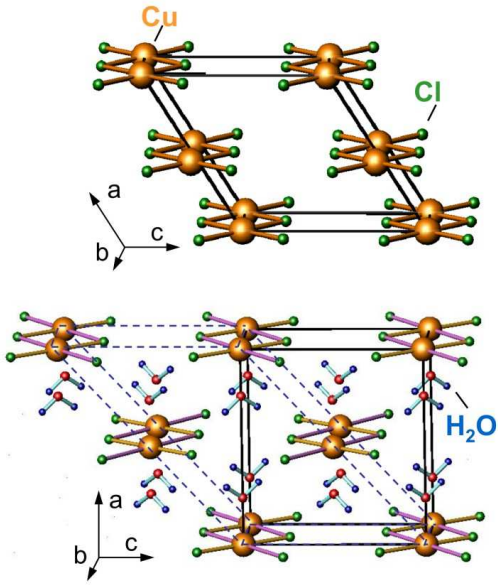


FIG. 1: (color online) Crystal structures of CuCl_2 (top) and $\text{CuCl}_2 \cdot 2\text{H}_2\text{O}$ (bottom). The shortest Cu–Cl bonds are highlighted (brown). The crystal water is intercalated between the CuCl_2 layers. The dashed line in the $\text{CuCl}_2 \cdot 2\text{H}_2\text{O}$ structure marks the unit cell of the water-free CuCl_2 .

the chains are modified. Whereas the structural changes can be easily understood by packing and electrostatics (negatively polarized O^{2-} is situated close to the Cu^{2+} ions, H^+ is attracted by Cl^-), the origin of the drastic change of magnetic properties – 1D versus 3D – is far from obvious. Unraveling the underlying microscopic physics is the aim of our joint theoretical and experimental study.

III. METHODS

Polycrystalline CuCl_2 was prepared by dehydration of $\text{CuCl}_2 \cdot 2\text{H}_2\text{O}$ (Alfa Aesar 99.999%) under vacuum at 390 K. Single crystals were grown by chemical transport in a temperature gradient from 650 K to 575 K with AlCl_3 (Alfa Aesar 99.999%, ultra dry) as transport agent. The chemical characterization of $\text{CuCl}_2 \cdot 2\text{H}_2\text{O}$ and of the CuCl_2 crystals was carried out by X-ray powder diffraction, DSC/TG-methods and chemical analysis. The heat of dehydration was determined by DSC.²⁹ Based on five independent measurements, the heat of dehydration is $\Delta H_{\text{dehyd.}}^0 = (117 \pm 2) \text{ kJ/mol}$ at 400 K.

Magnetization was measured in a SQUID magnetometer (1.8–300 K) in magnetic fields up to 7 T. Heat capacity was determined by a relaxation method in the same temperature range up to $\mu_0 H = 9 \text{ T}$.

Exact diagonalization (ED) of the J_1 – J_2 Heisenberg Hamiltonian has been performed on $N = 16$ sites clusters using the ALPS code.¹⁷ The low-temperature behavior

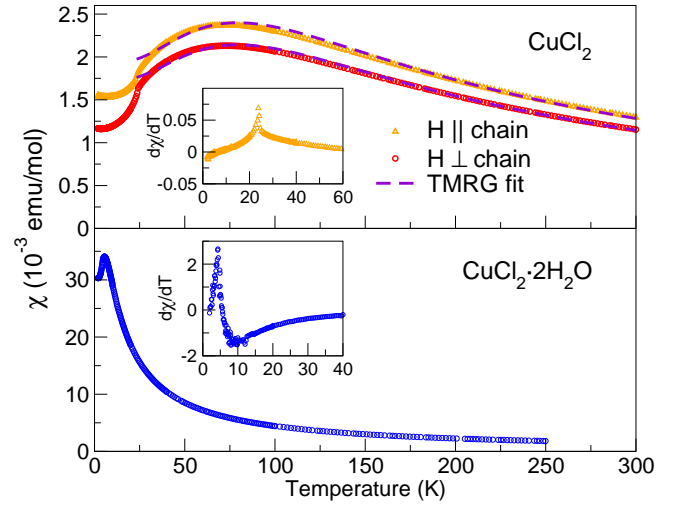


FIG. 2: (color online) Magnetic susceptibility of single crystalline CuCl_2 (top) and $\text{CuCl}_2 \cdot 2\text{H}_2\text{O}$ powder (bottom) as a function of temperature ($\mu_0 H = 1 \text{ T}$). TMRG fits are given by the dashed lines. The insets show the derivative $d\chi/dT$, the ordering temperatures are indicated by sharp peaks.

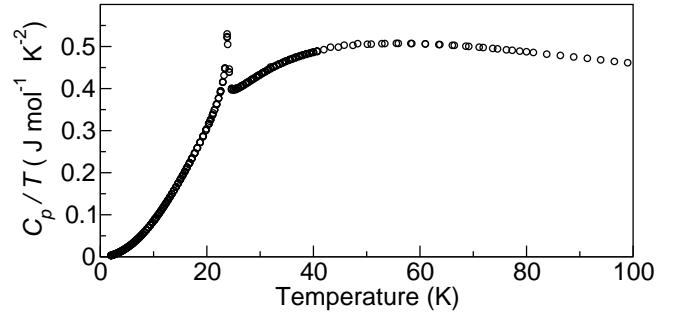


FIG. 3: Temperature dependence of the specific heat C_p/T of single crystalline CuCl_2 .

of the magnetic susceptibility has been simulated using the transfer-matrix density-matrix renormalization-group (TMRG) method.¹⁸

For the electronic structure calculations the full-potential local-orbital scheme FPLO (version: fplo7.00-28) within the local (spin) density approximation (L(S)DA) was used.¹⁹ In the scalar relativistic calculations the exchange and correlation potential of Perdew and Wang was chosen.²⁰ To consider the strong electron correlations for the $\text{Cu } 3d^9$ configuration, we use the LSDA+ U ²¹ approximation varying U_d in the physically relevant range from 6 – 8.5 eV. The LDA results were mapped onto an effective tight-binding model (TB) and subsequently to a Hubbard and a Heisenberg model.

IV. RESULTS AND DISCUSSION

A. Thermodynamic measurements

The susceptibility data for both compounds are shown in Fig. 2. CuCl_2 exhibits a broad maximum at $T_{\text{max}} \approx 75 \text{ K}$ as a fingerprint of quasi 1D behavior³⁰. An AFM Curie-Weiss temperature $\Theta_{\text{CW}} = +107 \text{ K}$ has been extracted from the high temperature region. A sharp kink at $T_N = 24 \text{ K}$ (see Fig. 2 and inset $d\chi/dT$) followed by a rapid drop of χ indicates a magnetic phase transition as earlier suggested.⁹

The measured zero-field specific heat as a function of temperature for CuCl_2 is shown in Fig. 3. Our data agree well with earlier studies.^{9,10} The specific heat curve shows a pronounced lambda shape anomaly at $T_N = 24 \text{ K}$ due to the onset of long range AFM ordering. The ordering temperature from C_p is in perfect agreement with T_N evaluated from susceptibility. Well below T_N the total specific heat is described by $C_p = \beta T^3$ with $\beta = 0.8514(3) \text{ mJ mol}^{-1} \text{ K}^{-1}$ (fit for $T < 10 \text{ K}$), indicating that both phononic and magnetic contributions to $C_p(T)$ are $\propto T^3$. The data in a field $\mu_0 H = 9 \text{ T}$ show no visible differences to the zero-field data.

In contrast to the quasi 1D susceptibility of CuCl_2 , the hydrated system shows an increasing χ down to low temperatures right above the AFM phase transition at 4.3 K (see Fig. 2 and inset $d\chi/dT$) in perfect agreement with earlier measurements.^{6,7} A Curie-Weiss temperature $\Theta_{\text{CW}} = +5.3 \text{ K}$ indicating weak AFM interactions has been evaluated.

B. Band structure calculations

The essentially different character of the susceptibility of both compounds points to a changed coupling regime rather than to a mere re-scaling according to the modified atomic distances. To construct an appropriate microscopic model based on the relevant interactions we perform *ab-initio* electronic structure calculations, as successfully demonstrated earlier for the closely related CuO_2 chain compound family^{11,12,13,16}.

Total and partial densities of states (DOS) for both compounds are pictured in Fig. 4. On a coarse energy scale both systems are similar, the contribution of the additional H states to the valence region is negligible. Both compounds show half-filled, well separated anti-bonding bands at the Fermi level. This metallic behavior is in contrast to the experiment and is a well known shortcoming of the LDA due to the underestimation of the strong Coulomb repulsion for the $\text{Cu}^{2+} 3d^9$ configuration. The observed insulating ground state is obtained (i) within the LDA+ U approximation or (ii) by a model approach mapping the relevant low lying LDA states onto an effective TB model, and, including the correlations, subsequently onto a Hubbard and a Heisenberg model.

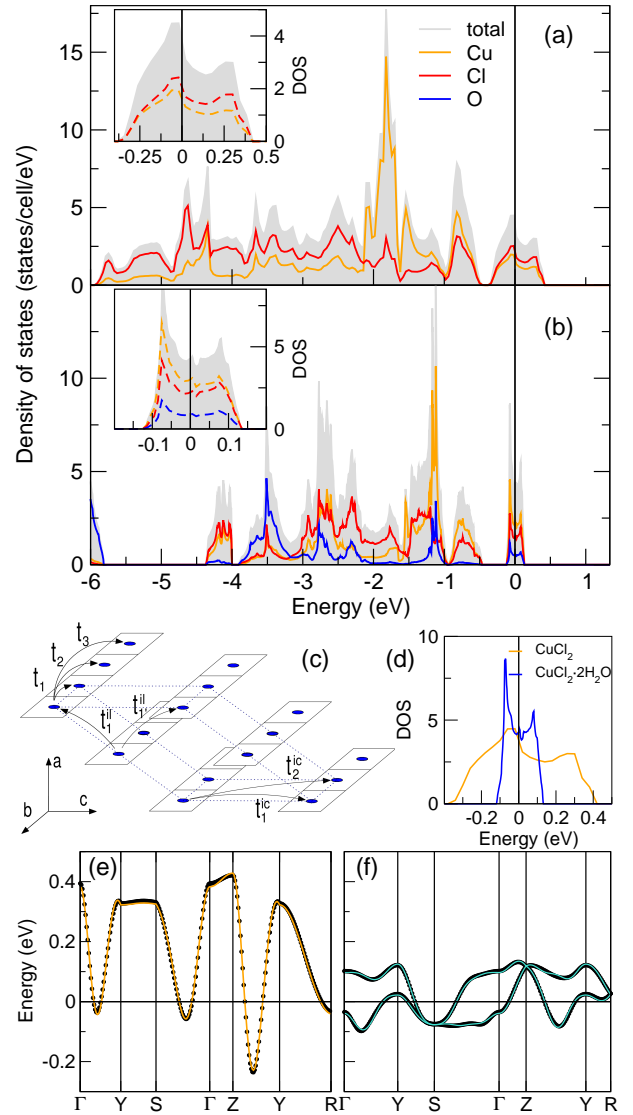


FIG. 4: (color online) Total and partial density of states and band structure of the anti-bonding band of CuCl_2 (a,e) and $\text{CuCl}_2 \cdot 2\text{H}_2\text{O}$ (b,f). The insets show the orbital character of the anti-bonding Cu-Cl (a) and Cu-Cl-O (b) states, respectively. The bandwidths are compared in (d). The fits (full lines (e,f)) of the TB model (c) are superimposed to the LDA band structures (circles (e,f)). The two bands in (f) originate from the two Cu atoms per cell in $\text{CuCl}_2 \cdot 2\text{H}_2\text{O}$.

A closer inspection of the DOS and the related band structure reveals two important differences: (i) Whereas the width of the anti-bonding band in CuCl_2 is 0.8 eV – rather typical for 1D edge-shared CuO_2 chains³¹ – the bandwidth in $\text{CuCl}_2 \cdot 2\text{H}_2\text{O}$ is reduced by more than a factor of three to about 0.25 eV (Fig. 4d). (ii) The magnetically active anti-bonding band in CuCl_2 is formed exclusively by Cu-Cl $dp\sigma$ states (inset Fig. 4a) corresponding to the bonds pictured in Fig. 1. In contrast, for $\text{CuCl}_2 \cdot 2\text{H}_2\text{O}$ the O $2p$ orbitals that are directed towards the Cu contribute significantly to this band (inset

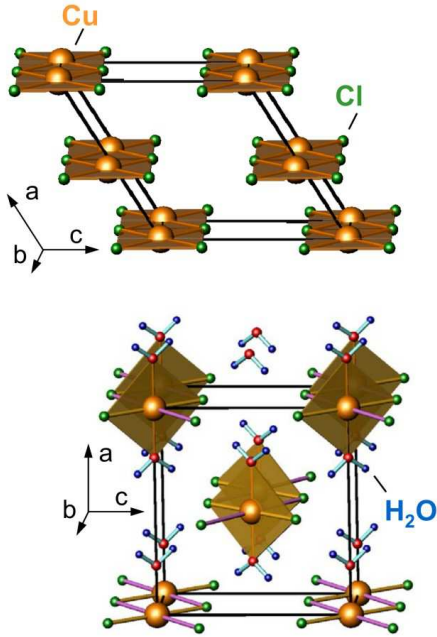


FIG. 5: (color online) Sketch of the magnetically active $p d \sigma$ -plaquette for CuCl_2 (top) and $\text{CuCl}_2 \cdot 2\text{H}_2\text{O}$ (bottom). Whereas these orbitals form quasi 1D edge shared chains in CuCl_2 , the plaquettes in $\text{CuCl}_2 \cdot 2\text{H}_2\text{O}$ are isolated resulting in weak, but 3D interactions.

Fig. 4b). This leads to the formation of a new $d p \sigma$ orbital perpendicular to the original ones. The related CuCl_4 or CuCl_2O_2 plaquettes are shown in Fig. 5. These plaquettes, relevant for the magnetic couplings, form edge-shared chains in CuCl_2 , whereas they are isolated in the hydrated system.

Naturally, this “orbital switching” induced by the crystal water implies a change of the coupling regime from 1D to 3D. To study these changes on a quantitative level, we constructed a TB model (Fig. 4c) for both compounds and fitted it to the relevant LDA bands (Fig. 4e,f). The leading transfer integrals t_i are given in Table I. The calculated t_i confirm the intuitive picture that corresponds to Fig. 5: CuCl_2 shows quasi 1D dispersion along the chain with dominating NNN hopping t_2 , and a considerably weaker coupling between the chains, while the coupling between adjacent layers is very small. On the other hand, the changed plaquette arrangement in $\text{CuCl}_2 \cdot 2\text{H}_2\text{O}$, induced by the crystal water, leads to a strongly reduced band width (Fig. 4d) and correspondingly small isotropic (3D) transfer integrals (Table I).

For the strongly correlated limit ($U_{\text{eff}} \gg t_i$) at half filling, the TB model can be mapped via a Hubbard model to a Heisenberg model with resulting AFM exchange couplings $J_i = 4t_i^2/U_{\text{eff}}$ where U_{eff} is the correlation in the effective one-band description. Depending on the choice of U_{eff} within a reasonable range^{3,16,22} ($U_{\text{eff}} = 3.5 - 4$ eV) this leads to exchange constants $J_i = 3 - 5$ K for the three leading couplings in $\text{CuCl}_2 \cdot 2\text{H}_2\text{O}$ (Table I).

t_i/meV	t_1	t_2	t_1^{ic}	t_2^{ic}	t_1^{il}
CuCl_2	34	117	61	-19	8
$\text{CuCl}_2 \cdot 2\text{H}_2\text{O}$	17	6	4	16	20

TABLE I: Calculated leading hopping integrals t_i for the effective TB model shown in Fig. 4c.

These J 's are perfectly in line with the experimentally observed $T_N = 4.3$ K as could be expected for an almost isotropic 3D coupling. For CuCl_2 , the leading NNN t_2 results in $J_2 = 160 - 180$ K. Although of the correct order of magnitude compared to T_{max} and Θ_{CW} , this would clearly exceed the “overall AFM coupling” in the compound without additional FM interactions. Sizable FM interactions are typical for close to 90° bond angles according to the Goodenough-Kanamori-Anderson rules²³ and therefore expected for the NN J_1 in CuCl_2 . For a quantitative estimate of the FM contributions to the leading J 's we apply LSDA+ U calculations for different spin arrangements in magnetic super cells.

Mapping the resulting total energy differences to the Heisenberg model, we obtain the following total exchange integrals ($U_d = 7 \pm 0.5$ eV)³²: $J_1 = -(150 \pm 10)$ K, $J_2 = 155 \pm 25$ K and $J_1^{\text{ic}} = 35 \pm 5$ K. Within the error bars, the latter two agree very well with the J values calculated from the corresponding t 's of the TB approach,³³ indicating that FM contributions beyond NN are rather small. In contrast, we find a large FM contribution of about 175 K to J_1 as expected from the Cu-Cl-Cu bond angle of 93.6° . The size of the FM contribution to J_1 fits well to related edge-shared CuO_2 chain compounds.^{12,16}

The resulting leading exchange interactions confirm the intuitive picture of a quasi 1D chain model compound with small inter-chain coupling, very similar to LiCu_2O_2 .^{13,14,15} Therefore, the magnetic ground state is mainly determined by the ratio $\alpha \equiv J_2/J_1$ of the frustrating main interactions along the chains. For CuCl_2 , we find $\alpha = -(1.0 \pm 0.1)$ and predict a ground state well in the helical ordered region of the J_1 - J_2 -phase diagram.

Thus, the dehydration of $\text{CuCl}_2 \cdot 2\text{H}_2\text{O}$ to CuCl_2 leads to a drastic change of the coupling regime from 3D to quasi 1D and a completely different ground state that can be traced back to a switch of the magnetically active orbital.

C. Model analysis of magnetic susceptibility

For an independent evaluation of the leading exchange interactions in CuCl_2 we simulated $\chi(T)$ within a spin-1/2 J_1 - J_2 Heisenberg model for various J_2/J_1 ratios using the TMRG technique and fitted the resulting $\chi^*(T/J)$ curves to the measured $\chi(T)$. Rather typical for the J_1 - J_2 Heisenberg model,^{14,15} we find two possible solutions for the fit: (i) $\alpha = +3.0$ with $J_1 = 120$ K and $J_2 = 40$ K (AFM solution) and (ii) $\alpha = -1.5$ with

$J_1 = -90$ K and $J_2 = 135$ K (FM solution). The FM solution (ii) is in rather good agreement with the estimates from our *ab-initio* calculations. The corresponding fits are shown in Fig. 2. The AFM solution (i) can be discarded regarding our calculational results and the close to 90° Cu-O-Cu bond angle.

In a naive approach, using the relation $\Theta_{\text{CW}} \approx 1/2(J_1 + J_2 + J_{\text{ic}})$,²⁴ the theoretically estimated $\Theta_{\text{CW}}^{\text{theo}} \approx +30 \pm 10$ K seems to be inconsistent with the experimental $\Theta_{\text{CW}} \approx +100$ K. Thus, we choose a more sophisticated procedure performing ED studies for the FM solution,³⁴ which yield the expected $\Theta_{\text{CW}} \approx 1/2(J_1 + J_2)$, but only at high temperatures $T > 10J_2$. Since this high temperature region is inaccessible to experiments, we choose a temperature window of the Curie-Weiss fit in order to obtain Θ_{CW} for the highest temperatures measured ($225 \text{ K} < T < 300 \text{ K}$ corresponding to $1.7J_2 < T < 2.2J_2$). Using J_1 and J_2 from the TMRG, we obtain $\Theta_{\text{CW}}^{\text{theo}} = +72$ K. The remaining difference between $\Theta_{\text{CW}}^{\text{theo}}$ and $\Theta_{\text{CW}}^{\text{exp}}$ of about 30 K corresponds in very good agreement to the inter-chain coupling J_{ic} of about 35 K neglected in the ED simulations.

D. Thermochemical properties

The dramatic effect of the dehydration of $\text{CuCl}_2 \cdot 2\text{H}_2\text{O}$ certainly raises the question whether this is really a typical dehydration process or if the involvement of the crystal water related oxygen in the magnetic exchange via covalent Cu-O bonds is an indication for a chemical reaction on a different energy scale. The dehydration enthalpy $\Delta H_{\text{dehyd.}}^0 = 117 \text{ kJ/mol}$ of $\text{CuCl}_2 \cdot 2\text{H}_2\text{O}$ is a typical (small) value for this class of materials.^{25,26} Our *ab-initio* estimate for the dehydration enthalpy yields $\Delta H_{\text{dehyd.}}^0 = 95 \text{ kJ/mol}$ which is in quite good agreement with the measured value, providing additional confidence to the reliability of the calculational procedure.

V. SUMMARY

In summary, our joint theoretical and experimental study provides a consistent explanation for the fundamentally different magnetic properties of $\text{CuCl}_2 \cdot 2\text{H}_2\text{O}$ and CuCl_2 . Whereas $\text{CuCl}_2 \cdot 2\text{H}_2\text{O}$ is a quite isotropic 3D AFM with small exchange couplings due to the orientation of neighboring isolated CuCl_2O_2 plaquettes, CuCl_2 can be well understood in terms of a 1D FM-AFM J_1 - J_2 chain model. This extension of the originally, critically discussed 1D AFM-NN only model⁹ re-establishes the pronounced 1D nature of the magnetism in CuCl_2 . The dramatic change of magnetic properties between both compounds can be traced back to a switch of the magnetically active orbital induced by crystal water. From our *ab-initio* calculations and model studies of the measured susceptibility using the transfer-matrix density-matrix renormalization-group and exact diagonalization techniques we predict a helical ground state and likely related multiferroic behavior for CuCl_2 driven by strong in-chain frustration originating from FM nearest neighbor and AFM next-nearest neighbor exchange interactions. Our study reveals that crystal water can have crucial influence on the electronic and magnetic properties of low dimensional magnets. More general, our work emphasizes that a transfer of model parameters from seemingly closely related systems is rather dangerous. The unaware neglect of this fact will lead to an at best inaccurate description of the physical properties in many cases.

We acknowledge R. Kremer for valuable discussions, T. Xiang for providing the TMRG code, and S. Müller for supporting DTA and DSC studies.

Note added in revision: While revising our manuscript, we learned that our magnetic model and predicted ground state was confirmed by an independent study.²⁷

- ¹ H. G. Heide, K. Boll-Dornberger, E. Thilo and E. M. Thilo, *Acta Cryst.* **8**, 425 (1955).
- ² C. Gros, P. Lemmens, K.-Y. Choi, G. Güntherodt, M. Baenitz and H. H. Otto, *Europhys. Lett.* **60**, 276-280 (2002).
- ³ H. Rosner, S.-L. Drechsler, K. Koepernik, R. Hayn, and H. Eschrig, *Phys. Rev. B* **63**, 073104 (2001).
- ⁴ H. H. Otto and M. Meibohm, *Z. Kristallogr.* **214**, 558 (1999).
- ⁵ O. Janson, J. Richter and H. Rosner, *Phys. Rev. Lett.* **101**, 106403 (2008).
- ⁶ J. van den Handel, H. M. Gijsman and N. J. Poulsen, *Physica XVIII*, **11** (1952).
- ⁷ W. Marshall, *J. Phys. Chem. Solids* **7**, 159 (1958).
- ⁸ L. J. DeJongh and A. R. Miedema, *Adv. Phys.* **23**, 1 (1974). Idem. *ibid.* **50**, 947 (2001).
- ⁹ J. W. Stout and R. C. Chrisholm, *J. Chem. Phys.* **36**, 979 (1962).

- ¹⁰ M. G. Banks, PhD. thesis 2007, Loughborough University.
- ¹¹ H. J. Xiang and M.-H. Whangbo, *Phys. Rev. Lett.* **99**, 257203 (2007).
- ¹² U. Nitzsche, S.-L. Drechsler and H. Rosner, to be published.
- ¹³ A. A. Gippius, E. N. Morozova, A. S. Moskvina, A. V. Zalesky, A. A. Bush, M. Baenitz, H. Rosner and S.-L. Drechsler, *Phys. Rev. B* **70**, 020406 (2004).
- ¹⁴ S.-L. Drechsler, J. Målek, J. Richter, A. S. Moskvina, A. A. Gippius and H. Rosner, *Phys. Rev. Lett.* **94**, 039705 (2005).
- ¹⁵ T. Masuda, A. Zheludev, A. Bush, M. Markina and A. Vasiliev, *Phys. Rev. Lett.* **94**, 039706 (2005).
- ¹⁶ S.-L. Drechsler, O. Volkova, A. N. Vasiliev, N. Tristan, J. Richter, M. Schmitt, H. Rosner, J. Målek, R. Klingeler, A. A. Zvyagin and B. Büchner, *Phys. Rev. Lett.* **98**, 077202 (2007).
- ¹⁷ A. F. Albuquerque, F. Alet, P. Corboz, P. Dayal, A.

- Feiguin, S. Fuchs, L. Gamper, E. Gull, S. Gürtler, A. Honecker, R. Igarashi, M. Körner, A. Kozhevnikov, A. Läuchli, S.R. Manmana, M. Matsumoto, I.P. McCulloch, F. Michel, R.M. Noack, G. Pawłowski, L. Pollet, T. Pruschke, U. Schollwöck, S. Todo, S. Trebst, M. Troyer, P. Werner and S. Wessel, J. Mag. Magn. Mater. **310**, 1187 (2007).
- ¹⁸ X. Wang and T. Xiang, Phys. Rev. B **56**, 5061 (1997).
- ¹⁹ K. Koepnik and H. Eschrig, Phys. Rev. B **59**, 1743 (1999).
- ²⁰ J. P. Perdew and Y. Wang, Phys. Rev. B **45**, 13244 (1992).
- ²¹ H. Eschrig, K. Koepnik, I. Chaplygin, J. Solid State Chem. **176**, 482 (2003).
- ²² H. Rosner, H. Eschrig, R. Hayn, S.-L. Drechsler and J. Málek, Phys. Rev. B **56**, 3402 (1997).
- ²³ J. Kanamori, Theor. Phys. (Kyoto) **17**, 177-190 (1957).
- ²⁴ D. C. Johnston, R. K. Kremer, M. Troyer, X. Wang, A. Klümper, S. L. Bud'ko, A. F. Panchula and P. C. Canfield, Phys. Rev. **61**, 9558 (2000).
- ²⁵ M. Taniguchi, M. Furusawa and Y. Kiba, J. Therm. Anal. Cal. **64**, 177 (2001).
- ²⁶ J. A. Lumpkin and D. D. Perlmutter, Thermochimica Acta **249**, 325 (1995).
- ²⁷ M. G. Banks, R. K. Kremer, C. Hoch, A. Simon, B. Oulad-diaf, J.-M. Broto, H. Rakoto, C. Lee and M.-H. Whangbo, arXiv: 0904.2929.
- ²⁸ These compounds are known as J_1 - J_2 chain models with FM NN and AFM NNN exchange, where the different J_2/J_1 ratios lead to different ground states.
- ²⁹ Netzsch DSC 204 thermocouple, platinum crucible, heating rate 10 K/min, dry argon atmosphere, 10 mg sample.
- ³⁰ The absence of an impurity related Curie tail at low temperatures indicates the high quality of the sample.
- ³¹ For comparison, CuGeO₃ shows a bandwidth of 0.95 eV for the anti-bonding band, CuSiO₃ about 0.65 eV and LiCuVO₄ about 0.7 eV.
- ³² The chosen region for U_d covers the experimental NN exchange J_1 in La₂CuO₄.
- ³³ This good agreement justifies *a posteriori* the transfer of the U_{eff} and U_d values from the CuO₂ chain compounds.
- ³⁴ Even for medium size clusters ($N = 16$), ED perfectly describes the high-temperature region of $\chi(T)$ which obeys a Curie-Weiss law.